Venusian "hot spots": Physical phenomenon and its quantification

V. P. Goncharov
Institute of Atmospheric Physics, Russian Academy of Sciences, 109017 Moscow, Russia

V. M. Gryanik
Alfred-Wegener-Institute for Polar and Marine Research, 27570 Bremerhaven, Germany
and Institute of Atmospheric Physics, Russian Academy of Sciences, 109017 Moscow, Russia

V. I. Pavlov
UFR de Mathématiques Pures et Appliquées, Université de Lille 1, 59655 Villeneuve d'Ascq, France
(Received 19 December 2001; published 12 December 2002)

An overall picture of the Venusian hot spots phenomenon is considered in the framework of the simplest conceptual models that admit the solutions in the form of steadily rotating "hot" vortices. Model assumptions take into account only those features of the middle atmosphere in the polar region of Venus that are supported by observational data and are essential for understanding the physical mechanism initiating similar vortices. The problem is analyzed in the framework of both the pointlike and petal-like models of cyclostrophic vortices. Interpretation of these models as an upper and lower bound of a complete theory allows one to find the region of existence of the regimes responsible for the Venusian hot spots and also to establish and assess numerically conditions under which such vortices can be formed. The emphasis is on a comparison of the theoretically established results with the observational data.

DOI: 10.1103/PhysRevE.66.066304 PACS number(s): 47.32.−y, 52.30.−q, 47.10.+g

I. INTRODUCTION

Earth and Venus have some similarities and dissimilarities in basic parameters [1]: the radii R are ~6360 and ~6052 km; gravity accelerations are ~9.8 and 8.9 $\mathrm{m\,s^{-2}}$ (at surface); surface temperatures are ~288 and ~730 K; pressures near surface are 0.1 and 9.2 Mpa; densities near surface are 1.23 and 65.0 $\mathrm{kg\,m^{-3}}$; rotation periods are 23.9 h (prograde) and 243 days (retrograde); overhead motions of the Sun are east to west for the Earth and west to east for Venus (inclinations of equator to orbit are ~23° and ~177°). The pressure scale heights H of the Earth's and Venusian atmospheres are ~8.4 and ~15.8 km i.e., $H \ll R$.

The circulation of the Venusian atmosphere has a number of peculiarities making it different from the atmosphere of the Earth (Golitsyn [2,3]; Schubert and co-workers [4,5]; Kerzhanovich *et al.* [6]). In the context of the problem considered in this paper most essential of them are the following.

(1) There is ample evidence (see Fig. 1) for two hot spots in the Venusian polar region near the cloud tops (at altitudes about 60 km). This phenomenon was discovered during IR remote sensing from Pioneer Venus spacecraft (Taylor *et al.* [7]) and was also observed during IR interferometer spectrometer studies on board Venera 15 and Venera 16 spacecrafts (Linkin *et al.* [8]). These hot spots located symmetrically relative to the pole with latitude about 75°–85° have a radius of about 5° and rotate about the pole with a period of $T_a \sim 3$ days (Taylor *et al.* [7], Schubert *et al.* [4]; Linkin *et al.* [8]).

(2) Most of the atmosphere in the lower and middle latitudes at altitudes of the main cloud layer (at altitudes about 60 km) rotates, outstripping the planet rotation (Kerzhanovich *et al.* [6]; Newman *et al.* [9]; Leovy [10]). This phenomenon, called super-rotation, manifests itself as a strong zonal circulation with velocities $u \sim 100\ \mathrm{m\,s^{-1}}$ at equator (see Fig. 2). Thus the rotation period of the Venusian atmosphere can be estimated at $T \approx 4$ days in contrast to 243 days for the planet rotation. The altitude dependence of angular velocity demonstrated in Fig. 3 has a maximum at heights near 65 km, followed by a slump at altitudes 65–70 km. The explanation of the zonal nature of the circulation with such large velocities in the Venusian atmosphere can be given within

FIG. 1. Brightness temperature isolines indicating a dipole structure of hot spots, as measured on Venus by Venera 15 (from Linkin *et al.* [8]).

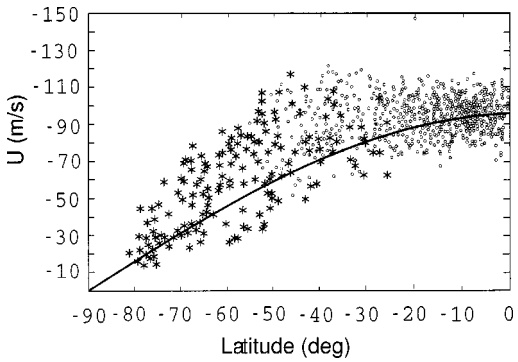

FIG. 2. Scatter of measurements of zonal circulation in the Venusian atmosphere (from Limaye [1]). For comparison, the solid line shows the latitude dependence of the zonal velocity on the assumption that the super-rotation of the Venusian atmosphere is characterized by a constant angular velocity.

the framework of the cyclostrophic balance suggested by Leovy [10]. The cyclostrophic balance implies the balance between meridional gradient of pressure and centrifugal force. After the mission of Pioneer Venus spacecraft this hypothesis has got an observational support (Schubert *et al.* [4]).

(3) At altitude $z \sim 60$ km, where hot spots are located, a polar atmosphere is appreciably colder than that at low latitudes, by $\sim 20-40$ K (Kerzhanovich *et al.* [6]; Schubert *et al.* [4]; Newman *et al.* [9]; Linkin *et al.* 1985 [8]; Yakovlev *et al.* [11,12]). Radio and infrared data for this altitude show essentially no change in the average temperature with latitude up to 55°. Next a temperature fall toward the pole becomes more appreciable and goes on in such a manner that a parabolic minimum is formed near the pole (see Fig. 4).

As was shown in papers of Gryanik [13] and Goncharov and Pavlov [14], the cyclostrophic balance (property 2), coupled with a meridional thermal contrast (property 3), can be used to explain the existence of stationary hot spots as a vortex structure (property 1). Indeed, as it has been mentioned above, localized temperature disturbances containing warmer and, correspondingly, lighter gas move in the field of centrifugal forces towards the axis of rotation, i.e., towards the pole. An accumulation of the warm gas at the pole results

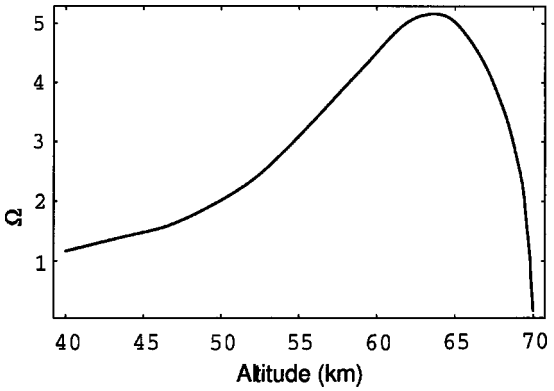

FIG. 3. The vertical profile of angular velocity of rotation of the Venusian atmosphere, Ω, in the polar region (reconstructed after data of Newman *et al.* [9]). The angular velocity is measured at 10^{-5} s^{-1}, the altitude at 1 km.

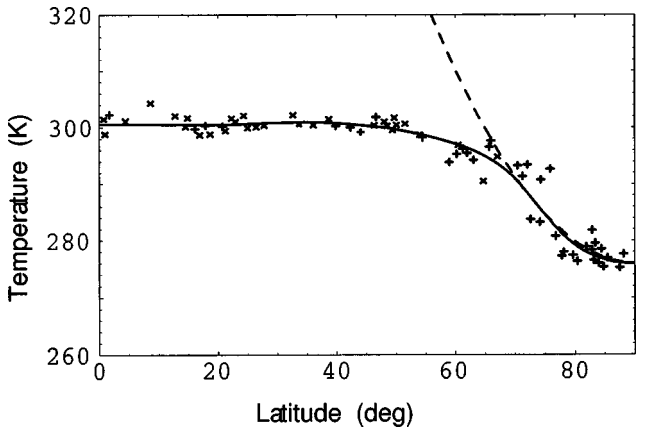

FIG. 4. Plot of temperature versus latitude, as defined at the 500 mbars level (from Newman *et al.* [8]). The dashed line illustrates the validity of a parabolic approximation near the pole.

in the formation of a polar hood. The colder disturbances move, correspondingly, away from the pole, which could result in the formation of a cold belt (a ''collar'') at a certain latitude if conditions prohibiting the transfer of disturbances down to an equatorial zone exist. Let temperature disturbances being warmer than an environment be vortical ones. In this case, the transfer of the parcels directly to a pole is in general not possible, because, near the pole, a vortex finds itself in a velocity field induced by another vortex and both vortices start to be involved in a mutual rotation around the pole. This could lead to the formation of a stationary ''dipole''-type vortex structure that rotates with an angular velocity different from the angular velocity of the zonal flow. Thus the existence of a warm polar hood, cold belt (a ''collar''), and hot spots (a ''dipole'') has a unified nature as a result of the separation of warm and cold gases in the field of centrifugal forces induced by the rotation of planetary atmosphere. Thermal hood and hot spots are formed at different altitudes. The hood is formed in layers where the vorticity is low enough and warm parcels may be transported directly to the pole; on the contrary, the vortical dipole is formed in the layer, where vorticity is high enough and warm parcels cannot move directly to the pole because of the interaction of vortices with each other. These vortices have principally nonlinear thermohydrodynamic nature.

It should be emphasized that the presence of localized vortices breaks zonal circulation in the polar region. In this sense, one can speak that the presence of vortices suggests the more complicated nature of dynamics in the polar regions of Venus as compared to the middle and lower latitudes. This motivates the interest to study the specifics of circulation in the polar region of Venus in more details.

Within the framework of dipole-vortex conception, Venusian hot spots can be characterized by four dimensional parameters: a relative angular velocity ω of rotation around the pole, a vortex intensity $\varkappa$, and two typical length scales l and a specifying a distance between vortices and their size, respectively. In turn, the basic state can be characterized by an angular velocity Ω of the super-rotation and by a length scale R_0 on which the thermal contrast between the pole and the equator occurs. Because, from a physical standpoint, the

problem is characterized by four dimensionless parameters: ω/Ω, l/R_0, a/l, $\varepsilon=\pi l^3\Omega(R_0\varkappa)^{-1}$, they must be connected by a relation

$$\varepsilon=F\left(\frac{\omega}{\Omega},\frac{l}{R_0},\frac{a}{l}\right). \tag{1.1}$$

Our aim is to investigate this relationship for two limiting cases: $a/l\ll 1$ when a model of localized pointlike vortices developed by Gryanik [13] is applicable and $a/l\sim 1$, $\Omega l(\omega R_0)^{-1}\gg 1$ when hot spots phenomenon can be analyzed in terms of petal-like vortices considered by Goncharov and Pavlov [14]. Using these extreme cases as an upper and lower bound of the theory, we intend in this paper to give a diagram of states showing the region of existence of possible regimes responsible for stationary rotating structures consisting of ''hot'' vortices of the dipole type and also to elucidate and to quantify conditions under which these vortices can be formed.

To this end, in Sec. II the conceptual model of cyclostrophic circulation in the Venusian polar region is introduced. In Sec. III a class of steady rotating vortex structures is considered. From them we study two types of dipolelike structures—localized point and petal vortices—in Sec. IV and V, respectively. Section VI contains the comparison of theoretical results with observational data and discussion.

II. CONCEPTUAL MODEL

Reasoning from above cited properties of the Venusian atmosphere dynamics, we present the simplest conceptual model that describes it as the dynamics of a two-dimensional incompressible fluid in a Cartesian coordinate system rotating about vertical axis x_3 with the constant angular velocity Ω. Because all dynamical variables of the problem are functions only of horizontal position vector $\mathbf{x}=\{x_1,x_2\}$, the basic equations of hydrothermodynamics in the field of centrifugal force (for a full derivation see Greenspan [15]) are

$$\partial_t v_i+v_k\partial_k v_i-2\Omega\varepsilon_{ik}v_k=-\rho^{-1}\partial_i p+\partial_i\Phi, \tag{2.1}$$

$$\partial_t T+v_k\partial_k T=0, \tag{2.2}$$

$$\partial_k v_k=0, \tag{2.3}$$

where v_i are components of a velocity field in the rotating coordinate system, ρ is fluid density, p is pressure, T is temperature, $\Phi=\frac{1}{2}\Omega^2 x_i^2$ is the potential of centrifugal force, and ε_{ik} is the alternating tensor ($+1$ for $ik=12$, -1 for $ik=21$, and zero for two indices being equal).

The energy equation (2.2) states that all heat exchanges are by convection; no conduction or heat sources being present. Proceeding from the incompressibility assumption, the fluid density ρ depends only on the temperature T but not on pressure p. Because this dependence is weak enough for the class of problems of interest here, we can use the approximation

$$\rho=\rho_0[1-\beta(T-T_0)], \tag{2.4}$$

where β is the coefficient of thermal expansion, ρ_0 is an undisturbed density, and T_0 is an undisturbed temperature.

Application of this system of equations to describe the hot spots dynamics in a polar region of the Venusian atmosphere means that we restrict our study to two-dimensional motions of enough large horizontal scale l and that vortex structures arise in a ''thin'' flat atmospheric layer near the 65 km altitude, where, as shown in Fig. 3, the angular velocity Ω of rotation remains practically constant.

The large-scale approximation also gives justification for using the model of an inviscid ideal fluid. Omitting viscous terms in Eq. (2.1) implies that frictional forces are negligible compared to the Coriolis force. For estimating the ratio of these forces, it is common practice to use the Ekman number $E=\frac{1}{2}\nu\Omega^{-1}l^{-2}$ where the quantity ν is considered as the coefficient of kinematic or turbulent viscosity. Because the angular velocity Ω of the Venusian atmosphere measures $(1-5)\times 10^{-5}\ \mathrm{s}^{-1}$, for $\nu\sim 10^{-6}-10^{-4}\ \mathrm{m}^2\,\mathrm{s}^{-1}$ and $l\sim 10-10^3$ km Ekman number falls in the range $E\sim 10^{-11}-10^{-3}\ll 1$.

For the undisturbed base state of the fluid when $\mathbf{v}=\mathbf{0}$, it follows from Eq. (2.1) the condition of *cyclostrophic balance*

$$\rho_0^{-1}\partial_i p_0=\Omega^2 x_i, \tag{2.5}$$

where p_0 is the background pressure.

Assuming that the departures of the pressure $p'=p-p_0$ and the density $\rho'=\rho-\rho_0=\rho_0\beta(T_0-T)$ from their undisturbed values p_0 and ρ_0 are small enough, i.e., $\beta(T_0-T)\ll 1$, we can use the Boussinesq approximation (see, for example, Turner [16]; Landau and Lifshitz [17]). This approximation implies that one may neglect the density variations and hence replace ρ by the constant value ρ_0, except in the ''buoyancy term'' $\rho'\partial_i\Phi/\rho_0$, where equation of state (2.4) must be used. As a result, Eq. (2.1) can be rewritten as

$$\partial_t v_i+v_k\partial_k v_i-2\Omega\varepsilon_{ik}v_k=-\rho^{-1}\partial_i p'+\Omega^2\beta(T-T_0)x_i, \tag{2.6}$$

$$\partial_t T+v_k\partial_k T=0,$$

$$\partial_k v_k=0.$$

To simulate the effect of increasing temperature from the pole to the equator, we take the background distribution of the temperature in the form

$$T_s(\mathbf{x})=T_0+\frac{\gamma}{2}\mathbf{x}^2,\quad \gamma>0. \tag{2.7}$$

This expression can be considered as an expansion of a radially symmetric stationary distribution $T_s(\mathbf{x})$ in the Taylor series in the vicinity of the pole.

The incompressibility condition (2.3) makes it possible to express velocity components in terms of the stream function ψ,

$$v_k=-\varepsilon^{ki}\partial_i\psi.$$

Taking the operator curl$=\varepsilon^{ki}\partial_i$ of Eq. (2.6) and thus excluding the pressure p' from the description, we obtain the coupled set of governing equations

$$\partial_t \Delta\psi+\varepsilon^{ik}\partial_i\psi\partial_k\Delta\psi=\Omega^2\beta\varepsilon^{ik}x_i\partial_k\tau,$$

$$\partial_t\tau+\varepsilon^{ik}\partial_i\psi\partial_k\tau=\gamma\varepsilon^{ik}x_i\partial_k\psi, \tag{2.8}$$

where $\Delta\psi$ is vorticity and $\tau=T-T_s$ is the temperature perturbation.

In the absence of temperature stratification ($\gamma=0$) and centrifugal force ($\Omega=0$), Eqs. (2.8) become traditional equations for the vortex evolution in a two-dimensional ideal fluid.

III. STEADILY ROTATING VORTEX STRUCTURES

Let us consider the solutions of Eqs. (2.8) which correspond to stationary vortex structures rotating with constant angular velocity ω around the pole.

Taking into account that when going to the new rotating coordinate system where the structures become immovable, the derivative with respect to time is transforming as

$$\partial_t=-\omega\varepsilon_{ik}x_i\partial_k,$$

we obtain the following system of equations:

$$\varepsilon_{ik}\frac{\partial}{\partial x_i}\left(\psi-\omega\frac{\mathbf{x}^2}{2}\right)\frac{\partial\Delta\psi}{\partial x_k}=\Omega^2\beta\varepsilon_{ik}x_i\frac{\partial\tau}{\partial x_k}, \tag{3.1}$$

$$\varepsilon_{ik}\frac{\partial}{\partial x_i}\left(\psi-\omega\frac{\mathbf{x}^2}{2}\right)\frac{\partial\tau}{\partial x_k}=\gamma\varepsilon_{ik}x_i\frac{\partial\psi}{\partial x_k}. \tag{3.2}$$

Rewriting Eq. (3.2) in the form

$$\varepsilon_{ik}\frac{\partial}{\partial x_i}\left(\psi-\omega\frac{\mathbf{x}^2}{2}\right)\frac{\partial}{\partial x_k}\left(\tau+\gamma\frac{\mathbf{x}^2}{2}\right)=0,$$

we find that

$$\psi-\omega\frac{\mathbf{x}^2}{2}=F\left(\tau+\gamma\frac{\mathbf{x}^2}{2}\right). \tag{3.3}$$

The function F can be found in an explicit form from the requirement that the flow in the background regime with no disturbances τ and ψ is also a solution of Eq. (3.3).

Inserting $\tau\equiv0$ and $\psi\equiv0$ in Eq. (3.3), we obtain

$$F(z)=-\frac{\omega}{\gamma}z, \tag{3.4}$$

and hence the functions ψ and τ are linearly related as

$$\psi=-\frac{\omega}{\gamma}\tau. \tag{3.5}$$

Using this relation in Eq. (3.2) gives the equation describing vortex structures in terms of stream function

$$\varepsilon_{ik}\frac{\partial}{\partial x_i}\left(\psi-\omega\frac{\mathbf{x}^2}{2}\right)\frac{\partial}{\partial x_k}\left(\Delta\psi-\frac{1}{R^2}\psi\right)=0, \tag{3.6}$$

where the length scale R, expressed as

$$R=R_0(\omega/\Omega),\quad R_0=(\beta\gamma)^{-1/2}, \tag{3.7}$$

is the dynamical characteristic of the model while R_0 is the thermal length scale characterizing the model in the background regime.

It should be emphasized that solutions of Eq. (3.6) corresponding to localized vortices exist only when $\gamma>0$. The physical meaning of this condition is that the field of centrifugal forces leads to the movement of colder (denser) fluid parcels away from the rotation axis, and an equilibrium other than a thermodynamic one may hold only in a case when temperature inhomogeneity supported by outer sources prohibits such movement, i.e., if temperature increases with the distance from the rotation axis: $\gamma>0$.

IV. LOCALIZED POINTLIKE VORTICES

Let us consider solutions of Eq. (3.6) describing a radially symmetric vortex dipole with center in the pole

$$\Delta\psi-R^{-2}\psi=\varkappa[\delta(z-z_0)+\delta(z-z_0^*)]. \tag{4.1}$$

Here $\delta(z)$ is the Dirac delta function, $\varkappa$ are vortex intensities ($\varkappa>0$ if the circulation is counterclockwise), $z_0=e^{i\theta}l/2$, and $z_0^*=-e^{i\theta}l/2$ are coordinates of vortices in the complex plane $z=x_1+ix_2$. It follows from Eq. (4.1) that the flow induced by such vortices is expressed in terms of the Green function $G(z)$ of the operator $(\Delta-R^{-2})$

$$\psi=\varkappa[G(|z-z_0|)+G(|z-z_0^*|)], \tag{4.2}$$

$$G(|z|)=-\frac{1}{2\pi}K_0\left(\frac{|z|}{R}\right), \tag{4.3}$$

where $K_n(x)$, $n=0,1,...$ is the modified Bessel function of nth order.

Substituting Eqs. (4.1) and (4.3) into Eq. (3.6) and equating terms with δ function and its derivatives, we obtain the condition connecting parameters of vortices with the angular velocity of their rotation:

$$\omega l=\frac{\varkappa}{\pi R}K_1\left(\frac{l}{R}\right), \tag{4.4}$$

where R as the function of ω is given by Eq. (3.7).

As shown by Gryanik [13], Eq. (4.4) can be rewritten in terms of the dimensionless parameters ξ and ε,

$$\varepsilon=\frac{\pi l^3\Omega}{R_0\varkappa},\quad \xi=\frac{\Omega l}{\omega R_0}, \tag{4.5}$$

as the equation

$$\varepsilon=\xi^2K_1(\xi). \tag{4.6}$$

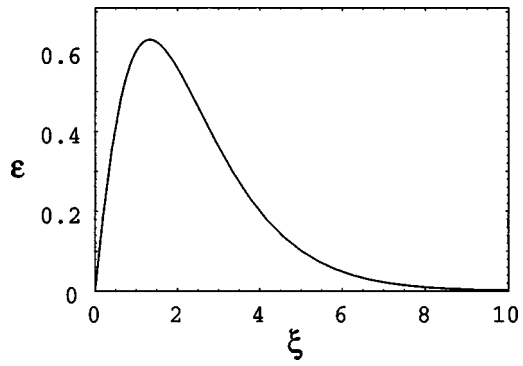

FIG. 5. The parameter ε as the function of ratio of angular velocities of rotation Ω/ω for the pointlike model.

The plot corresponding to this equation is presented in Fig. 5 and later will be treated (see Sec. VI) as a lower bound for the basic relation (1.1). Among other things, this plot indicates the law whereby the quantity ε characterizing a vortex intensity depends on the parameter Ω/ω, when the ratio l/R_0 is fixed.

In accordance with Fig. 5, it is clear that for each fixed ε Eq. (4.6) has two roots $\xi_{\pm}$ if $\varepsilon<\varepsilon_*$, one root ξ_* if $\varepsilon=\varepsilon_*$, and no roots if $\varepsilon>\varepsilon_*$, where ε_* is the threshold value of the parameter ε. The numerical computation gives $\varepsilon_*\approx 0.63$ and $\xi_*\approx 1.38$. Thus a point-vortex dipole can exist only if

$$\frac{\pi l^3\Omega}{R_0\varkappa}\leqslant\varepsilon_*\approx 0.63. \tag{4.7}$$

If the angular velocity of rotation Ω is fixed inequality (4.7) shows that either vortices should be sufficiently intense $\varkappa\geqslant\varkappa_*=\pi l^3\Omega R_0^{-1}\varepsilon_*^{-1}$, or distance between them should not exceed a limiting value $l\leqslant l_*=(\pi)^{-1/3}(R_0\varepsilon_*\varkappa/\Omega)^{1/3}$. The threshold value of the intensity of vortices increases with increasing of angular velocity of rotation $\varkappa_*\sim\Omega$ while the limiting distance decreases: $l_*\sim\Omega^{-1/3}$. The threshold value of the intensity of vortices decreases with the decreasing of temperature inhomogeneity $\varkappa_*\sim\gamma^{-1/2}$ but the limiting distance increases: $l_*\sim\gamma^{1/6}$.

V. PETAL-LIKE VORTICES

Solutions considered in this section look like two-petal regions bounded by a closed contour such that the quantity $q=\Delta\psi-R^{-2}\psi$ takes constant values q_0 and 0, respectively, inside and outside the region (details of the contour dynamics method and of the operator techniques can be found in Refs. [18], [19]). Analytic representations of such solutions in the complex z plane are given by the contour integral

$$q=\frac{q_0 i}{2\pi}\oint ds\,\frac{\hat{z}_s}{z-\hat{z}}, \tag{5.1}$$

which is taken around the closed contour $z=\hat{z}(s)$, where s is contour arc length.

Because the vector $\hat{z}_s=\partial\hat{z}/\partial s$ is tangential to the contour and the normalizing condition $|\hat{z}_s|^2=1$ holds, we can write that

$$\hat{z}_s=e^{i\varphi}, \tag{5.2}$$

where φ is the inclination angle of the tangent to the contour in a point s.

The equation for finding the contour shape is most conveniently formulated in terms of a contour curvature κ that is related with the inclination angle φ as

$$\kappa=\partial_s\varphi. \tag{5.3}$$

Referring to Goncharov and Pavlov [14] for more details, we present here the summary results on describing a contour shape in a weak-curvature approximation when the stream function $\hat{\psi}(s)$ on the contour and the curvature $\kappa(s)$ are connected by simple local relation (Appendix A)

$$\hat{\psi}(s)=\frac{q_0R^3}{4}\kappa(s), \tag{5.4}$$

and κ is governed by the equation (Appendix B)

$$\left(\frac{\partial\kappa}{\partial s}\right)^2=-\frac{1}{4}\kappa^4+c_1\kappa^2+d^{-3}\kappa+c_2. \tag{5.5}$$

Here c_1 and c_2 are two dimensional constants parametrizing the solutions, and the scale d is given by

$$d=\frac{R}{2}\left(\frac{q_0}{\omega}\right)^{1/3}. \tag{5.6}$$

Within a class of self-nonintersecting contours, Eq. (5.5) has the periodic solution expressed in terms of elliptic sn functions as

$$\kappa=\frac{1}{d}\left(b+\frac{a-b}{1-\alpha\,\mathrm{sn}\left(\dfrac{\lambda}{d}s\middle|m\right)}\right), \tag{5.7}$$

where parameters a, b, λ are related to the independent basic parameters α and m,

$$\begin{aligned}
a&=-2^{-1/3}\frac{\alpha(1+m-2\alpha^2)}{[(1-m)^2\alpha(m-\alpha^4)]^{1/3}},\\
b&=2^{-1/3}\frac{\alpha^2+m(\alpha^2-2)}{\alpha[(1-m)^2\alpha(m-\alpha^4)]^{1/3}},\\
\lambda&=2^{-1/3}\frac{\sqrt{(\alpha^2-m)(1-\alpha^2)}}{[(1-m)^2\alpha(m-\alpha^4)]^{1/3}}.
\end{aligned} \tag{5.8}$$

In turn, the parameters c_1 and c_2 are expressed in terms of a and b as

$$c_1=d^{-2}\left(\frac{ba}{2}-\frac{1}{a+b}\right),\quad c_2=-\frac{d^{-4}}{4}(b+a+b^2a^2). \tag{5.9}$$

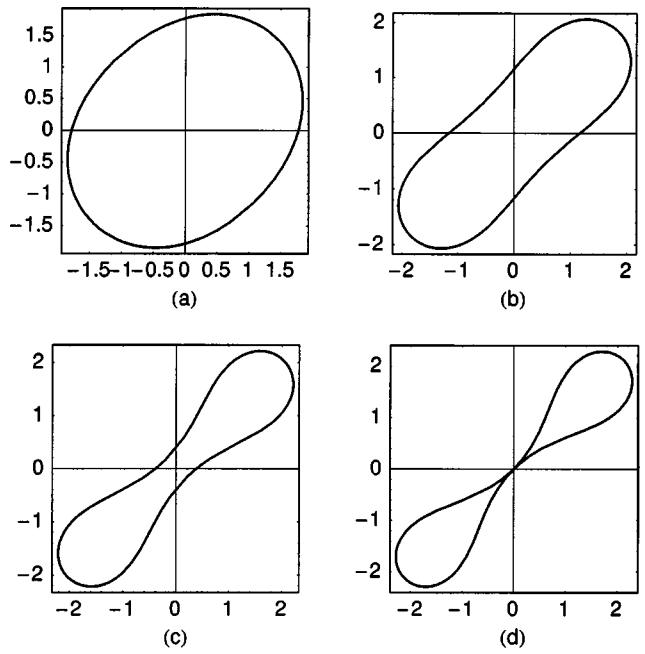

FIG. 6. Double-petal vortex structures in the plan of $z=x_1+ix_2$: $\alpha=0.05$ (a); $\alpha=0.20$ (b); $\alpha=0.30$ (c); $\alpha=0.35$ (d). The points s_+ lie in the petal tips and s_- lie between the petals.

The equations describing the boundary shape of vortex structures rotating in the z plane can be obtained by integrating Eq. (5.2). It can be directly verified that if κ satisfies Eq. (5.5), the solution of Eq. (5.2) is given by

$$\hat{z}(s)=2d^3\left[\frac{\partial\kappa}{\partial s}+i\left(c_1-\frac{\kappa^2}{2}\right)\right]e^{i\varphi}, \tag{5.10}$$

where in turn the inclination angle can be found by integrating expression (5.3) along a contour:

$$\varphi(s)=\int^s ds'\,\kappa(s')=\frac{b}{d}s+\frac{a-b}{\lambda}\Pi\left(\alpha^2,\mathrm{am}\left(\frac{\lambda}{d}s|m\right)|m\right) -2\,\mathrm{Im}\ln\left[\mathrm{cn}\left(\frac{\lambda}{d}s|m\right)\sqrt{\alpha^2-m}+i\,\mathrm{dn}\left(\frac{\lambda}{d}s|m\right)\sqrt{1-\alpha^2}\right]. \tag{5.11}$$

Here $\Pi(u;\vartheta|m)$ is the incomplete elliptic integral of the third kind and $\mathrm{am}(u|m)$ is the Jacobi amplitude.

From Eq. (5.7), it is clear that the contour curvature of the two-petal structure, being an oscillatory periodic function with period $4K(m)/\lambda$, has extrema at the points

$$s_-=(4j-1)d\frac{K(m)}{\lambda},\quad s_+=(4j-3)d\frac{K(m)}{\lambda},\quad j=1,2,$$

where $K(m)$ is the complete elliptic integral of the first kind [20]. The tops of the petals lie at the point s_+ and the point s_- are in the troughs between the petals. Examples of two-petal structures are illustrated in Fig. 6 for various values of the parameter α.

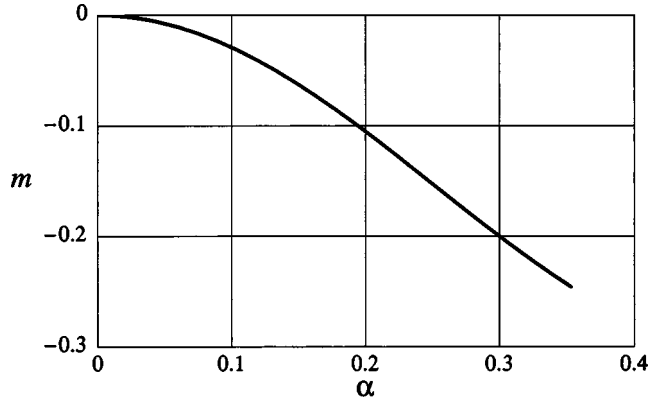

FIG. 7. The dependence $m(\alpha)$ for the two-petal vortex regime. Marginal point ($\alpha=0.35$, $m=-0.25$) corresponds to limit vortex structure with a self-contact contour.

As analysis of Eq. (5.11) shows, because a contour of a two-petal vortex structure is closed, we must satisfy the condition

$$bk(M)+(a-b)\Pi(\alpha^2|m)=-\frac{\pi}{4}\lambda, \tag{5.12}$$

where $\Pi(u|m)=\Pi(u;(\pi/2)|m)$ is the complete elliptic integral of the third kind.

Equation (5.12) enable us to compute the dependence $m(\alpha)$ displayed in Fig. 7 as a curve that has a limit point ($\alpha=0.353$, $m=-0.246$) where the contour of the vortex structure becomes self-contacting.

Distances of points s_+, s_- from the coordinate origin are given by

$$\rho_+=2^{1/3}d\frac{-m(1+2\alpha)+\alpha^3(\alpha+2)}{[(1-m)\alpha^2(\alpha^4-m)^2]^{1/3}},$$

$$\rho_-=2^{1/3}d\frac{-m(1-2\alpha)+\alpha^3(\alpha-2)}{[(1-m)\alpha^2(\alpha^4-m)^2]^{1/3}}. \tag{5.13}$$

Being functions of α, ρ_+ and ρ_- identify the maximal and minimal sizes of vortex structure, respectively.

The self-contacting occurs when $\rho_-=0$. Together with Eq. (5.12) this gives all the necessary conditions to compute the marginal value $\rho_+^*/d=2.99$.

This extreme case can be used to estimate an upper bound for the basic relation (1.1). The result to be expected is evidently applicable when $a/l\sim 1$ and $\xi=\Omega l(\omega R_0)^{-1}\gg 1$, i.e., when a finite size vortex can be described in a weak-curvature approximation. The corresponding expression can be easily obtained from Eq. (5.6) if we take into account that

$$q_0=\frac{\varkappa}{S}, \tag{5.14}$$

where $\varkappa$ and S are the vortex intensity of an isolated petal and its area, respectively.

Because in the limiting case [see Fig. 6(d)] the typical size l and the area S are approximately estimated as

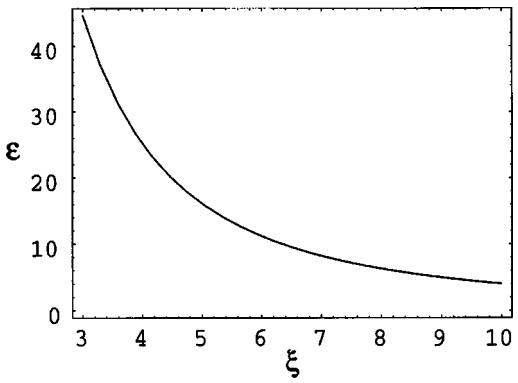

FIG. 8. Plot of quantity ε versus parameter ξ for the petal-like model.

$$l=4d, \quad S=d^2, \tag{5.15}$$

from Eq. (5.6) it follows that

$$\left(\frac{l}{R}\right)^3=\frac{128\varkappa}{l^2\omega}. \tag{5.16}$$

After reformulation in terms of parameters ε and ξ defined as before by Eq. (4.5), Eq. (5.16) gives the law

$$\varepsilon=\frac{128\pi}{\xi^2}, \tag{5.17}$$

which is plotted in Fig. 8.

VI. DISCUSSION AND CONCLUSIONS

First and foremost we sum up those conclusions about properties of hot spots in the polar region of Venus which are in a qualitative agreement with both the discussed theoretical models. Some quantitative estimates of structural and dynamic parameters of the dipole are given as well.

(1) The hot spots are dipolelike vortical structures consisting of two vortices of an equal intensity. Being symmetrically located at equal distances from the pole, these vortices rotate around it with a constant angular velocity (Taylor *et al.* [7]).

(2) The hot vortex spots cannot penetrate to altitudes $z>70$ km. This is due to the character of a meridional temperature inhomogeneity in the polar region. Because at heights $z>70$ km the temperature decreases from the pole toward the equator (Newman *et al.* [9]; Linkin *et al.* [8]) and hence $\gamma<0$, Eqs. (2.8) do not have localized vortical solutions in this case. Moreover, as can be shown, if $\gamma<0$ the cyclostrophic instability does not develop. The vortices seem to be localized in the layer $55<z<65$ km. This is suggested by the character of vertical distribution of vorticity in the polar region (see Fig. 3).

In order that temperature data characterizing the structure of hot spots can be used for quantitative estimates, the vortical parameters q_0 and $\varkappa$ should be expressed in terms of thermal ones. This provides a possibility to indirectly estimate the quantities ξ, ε which were arising in previous sections under theoretical studying.

This task turns out to be sufficiently simple for the model of petal-like vortices. Because the model exploits the approximation $d/R\gg 1$, the corresponding estimations can be easily obtained from the relationship

$$\Delta\psi-R^{-2}\psi=q_0, \tag{6.1}$$

which holds throughout the vortex core.

Ignoring the first term in Eq. (6.1) and taking into account Eq. (3.5) together with the relation

$$\beta\approx 1/T_0, \tag{6.2}$$

where T_0 is the pole temperature, at the second approximation in the small parameter R/d we can find the evaluation

$$q_0=\frac{\Omega^2}{\omega}\,\frac{\tau_m}{T_0}, \tag{6.3}$$

where τ_m is the amplitude of the temperature deviation in the hot spot against the background T_s.

Substitution of Eqs. (6.3) and (5.15) into Eq. (5.6) gives

$$\frac{\omega}{\Omega}=\left(\frac{l}{2R_0}\right)^3\frac{T_0}{\tau_m}, \tag{6.4}$$

where the temperature ratio τ_m/T_0 emerges instead of the parameter q_0/Ω.

From Eqs. (6.3) and (6.4) we can deduce one more important property supported by observations (Schubert *et al.* [4]; Taylor *et al.* [7]; Linkin *et al.* [8]). Because the vortex spots are hot and hence the temperature deviation τ_m is positive, the quantities ω and q_0 must have the same sign as the angular velocity Ω of rotation. Therefore the hot spots have the same sense of rotation as the Venusian atmosphere and outstrip it.

In order that the point-vortex model could also be interpreted in terms of the thermal structure of hot spots, we must extend the results of Sec. IV to dipoles composed of finite-size vortices. To do this, we assume that the vortices have circular cores of an equal radius a and that the quantity q is kept constant, taking values q_0 and 0, respectively, inside and outside the vortex core.

If we assume further that the size of the vortices is much less than the intervortical distance l but is much more than the screening radius R, i.e.,

$$R\ll a\ll l,$$

and neglect core's deformations arising only in the fifth order of the perturbation theory in the small parameter a/l, we can then conclude that the result (6.3) remains valid at the second approximation in the small parameter R/a.

Equation (6.3) enables us to use measuring data characterizing thermal structure of hot spots in order to estimate the parameter ε for the theory of both pointlike and petal-like vortices.

From Eq. (4.5), with the help of Eq. (5.14), we can find

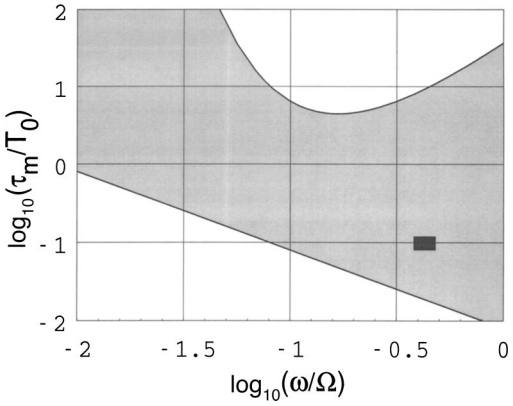

FIG. 9. Domain of existence of hot spots phenomenon. The upper curve (point vortices) is calculated from Eq. (6.6) and the down one (patches) is calculated from Eq. (6.7). The values of parameters are given in text. The dark rectangle marks the range of experimental parameters.

$$\varepsilon = \frac{\pi l^3}{S R_0} \frac{\omega}{\Omega} \frac{T_0}{\tau_m}, \tag{6.5}$$

where depending on the choice of model the vortex core area S takes values $S=\pi a^2$ for the point model and $S=l^2/16$ for the petal one.

Because comparisons of theoretical results with experimental data are more convenient in terms of the parameters τ_m/T_0 and ω/Ω, after reparametrization of Eqs. (4.6) and (5.17) we obtain the relations

$$\frac{\tau_m}{T_0} = \frac{l R_0}{a^2} \left(\frac{\omega}{\Omega} \right)^3 K_1^{-1} \left(\frac{l}{R_0} \frac{\Omega}{\omega} \right), \tag{6.6}$$

$$\frac{\tau_m}{T_0} = \frac{1}{8} \left(\frac{l}{R_0} \right)^3 \frac{\Omega}{\omega}, \tag{6.7}$$

which are used as upper and lower bounds of the theory.

Following the factual evidence (see, for example, Linkin *et al.* [8]), to make estimates we take values $\gamma \approx 2 \times 10^{-6}\ \mathrm{K\,km^{-2}}$, $l \approx 2 \times 10^3$ km, $T_0 \approx 250$ K, and $a \approx 500$ km, which are typical for the Venusian atmosphere. As $\beta \approx 1/T_0$, the thermal scale can be estimated in accordance with Eq. (3.7) as $R_0 \approx 10^4$ km.

Plugging the parameters l, a, and R_0 in Eqs. (6.6) and (6.7), we find the domain of natural physical parameters τ_m/T_0 and ω/Ω (see Fig. 9) where the Venusian hot spots phenomenon can be explained within the framework of cyclostrophic vortex theory.

As may be inferred from Fig. 9, the upper bound determined by the point-vortex model can be unlikely attained due to the inequality $\tau_m \ll T_0$.

To show the location of the Venusian hot spots phenomenon in Fig. 9, we estimate the range of typical parameters τ_m/T_0 and ω/Ω, using reliable experimental data. According to this data (Taylor *et al.* [7]; Linkin *et al.* [8]), the rotation period T_a of the Venusian hot spots ranges from 2.7 to 2.9 days while the super-rotation period is estimated at $T_{atm} = 4$ days.

As the quantity ω is the relative angular velocity of the hot spots rotation, it is determined as the difference

$$\omega = |\Omega - \omega_a|,$$

where $\Omega = 2\pi/T_{atm}$ and $\omega = 2\pi/T_a$ are the absolute angular velocities of rotations for the atmosphere and the hot spots, respectively. Thus we find that the parameter ω/Ω falls in the range 0.38–0.48.

Assuming that reasonable values of τ_m lie in the range 20–30 K, we obtain the domain marked in Fig. 9 by the dark rectangle. Its location clearly indicates that although both of our models are far from the hot spots phenomenon observed in the Venusian atmosphere, they serves as upper and lower bounds. For a more exact quantitative description, there is a need to develop intermediate models where the parameter a/l would take values between 0 and 1.

The petal-like model allows us to estimate the influence of the vortex dipoles on the zonal circulation. After averaging Eq. (6.1) over latitude ϑ, we find

$$\left(\frac{1}{r} \frac{\partial}{\partial r} r \frac{\partial}{\partial r} - \frac{1}{R^2} \right) \overline{\psi} = \frac{2 q_0}{\pi} \vartheta(r), \tag{6.8}$$

where $\overline{\psi}$ is the latitude-averaged stream function,

$$\overline{\psi} = \frac{1}{2\pi} \int_0^{2\pi} \psi d\vartheta, \tag{6.9}$$

and $\vartheta(r)$ is the petal shape in the polar coordinates r, ϑ.

Using the stream function $\overline{\psi}$, we can compute the mean zonal velocity as

$$u = \Omega r + \frac{\partial \overline{\psi}}{\partial r}, \tag{6.10}$$

where the first term describes solid-state rotation with the angular velocity Ω and the second one is the dipole contribution to the zonal circulation.

The results of numerical calculations, in accordance with Eqs. (6.8) and (6.10), under conditions

$$\left. \frac{\partial \overline{\psi}}{\partial r} \right|_{r=0} = 0, \quad \left. \frac{\partial \overline{\psi}}{\partial r} \right|_{r=\infty} = 0,$$

are shown in Fig. 10 where parameters l, R_0, τ_m, T_0 take the following typical values: $l = 2 \times 10^3$ km, $R_0 = 10^4$ km, $\tau_m = 25$ K, and $T_0 = 250$ K.

ACKNOWLEDGMENTS

This work was partly supported by the Russian Foundation for Basic Research (Grant No. 00-05-64019-a). The authors thank G. Golitsyn and N. Schorghofer for useful comments.

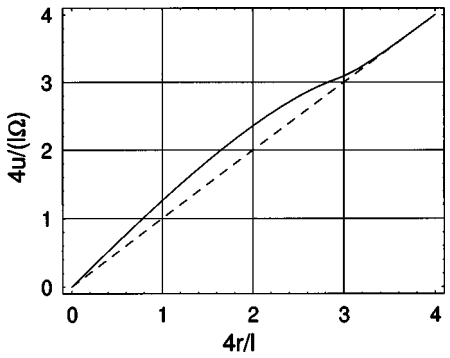

FIG. 10. The influence of hot spots on the mean zonal velocity. The dashed line corresponds to the rotational motion with constant angular velocity.

APPENDIX A: RELATIONSHIP BETWEEN THE STREAM FUNCTION AND CURVATURE ON THE BOUNDARY OF THE DOMAIN

We find the equation

$$\varepsilon_{ik}\frac{\partial}{\partial x_i}\left(\psi-\omega\frac{r^2}{2}\right)\frac{\partial}{\partial x_k}\left(\Delta\psi-\frac{\Omega^2\gamma\beta}{\omega^2}\psi\right)=0 \qquad \text{(A1)}$$

for the quantity

$$q=\Delta\psi-R^{-2}\psi, \quad R=\frac{|\omega|}{\Omega\sqrt{\gamma\beta}}, \qquad \text{(A2)}$$

where R is the length-scale characteristic of the problem.

The spatial distribution of the quantity q is supposed to be given by a piecewise uniform function in the plane $z=x_1+ix_2$. Let us note again that $\mathbf{x}=\{x_1,x_2\}$. Such a distribution may be described simply using the two-dimensional Heaviside step functions: $\theta(z)=1$, if $z\in D$, and $\theta(z)=0$, if $z\notin D$. Here, D is a singly connected region in the z plane bounded by a closed contour, which is given in the parametric form

$$z=\hat{z}(s), \qquad \text{(A3)}$$

where s is contour arc length. In terms of θ functions, the distribution q of interest can be written as

$$q=q_0\theta(z), \qquad \text{(A4)}$$

where q_0 is a constant value that the quantity q takes within region D.

For the vector $\hat{z}_s=\partial\hat{z}/\partial s$ tangential to the contour, the following normalizing condition holds:

$$|\hat{z}_s|^2=1. \qquad \text{(A5)}$$

The θ functions admit the following analytical representation through the contour integral:

$$\theta(z)=\frac{i}{2\pi}\oint ds\,\frac{\hat{z}_s}{z-\hat{z}}. \qquad \text{(A6)}$$

Using the formula (see Ref. [21]) that can be obtained as a corollary of the Cauchy's formula in the theory of function of complex variable

$$\frac{\partial}{\partial\bar{z}}\frac{1}{z}=\pi\delta(\mathbf{x}),$$

the z derivative of the θ function can be easily calculated from Eq. (A6) as

$$\frac{\partial\theta}{\partial\bar{z}}=\frac{i}{2}\oint ds\,z_s\delta(\mathbf{x}-\hat{\mathbf{x}}). \qquad \text{(A7)}$$

Here, $z=x_1+ix_2$, $\bar{z}=x_1-ix_2$. The substitution of Eq. (A4) in Eq. (A1), after differentiating θ functions using Eq. (A7), leads to the contour integral

$$\begin{aligned}\varepsilon_{ik}\frac{\partial}{\partial x_i}\left(\psi-\omega\frac{r^2}{2}\right)\frac{\partial}{\partial x_k}\left(\Delta\psi-\frac{1}{R^2}\psi\right)&\\ =-4q_0\left[\frac{\partial\theta}{\partial z}\frac{\partial}{\partial\bar{z}}\left(\psi-\omega\frac{r^2}{2}\right)\right]&\\ =q_0\oint ds\,\delta(\mathbf{x}-\hat{\mathbf{x}})\frac{\partial}{\partial s}\left(\hat{\psi}-\omega\frac{|\hat{z}|^2}{2}\right)=0. \qquad \text{(A8)}\end{aligned}$$

From this it follows that the rotating-frame stream function must be constant on the vortex boundary:

$$\hat{\psi}-\omega\frac{|\hat{z}|^2}{2}=\text{const.} \qquad \text{(A9)}$$

Here, $\hat{\psi}$ is defined by $\hat{\psi}=\psi_{\mathbf{x}=\hat{\mathbf{x}}}$.

Equation (A9) determines the boundary shape (A3) if the stream function $\hat{\psi}$ is expressed in terms of the contour coordinates $\hat{\mathbf{x}}$. Taking into account that Green's function $G(\mathbf{x},\mathbf{x}')$ of operator $\Delta-R^{-2}$ is given by

$$G(\mathbf{x},\mathbf{x}')=-\frac{1}{2\pi}K_0\left(\frac{|\mathbf{x}-\mathbf{x}'|}{R}\right),$$

and solving Eq. (A2), we obtain the stream function ψ in terms of q:

$$\psi(\mathbf{x})=-\frac{1}{2\pi}\int d\mathbf{x}'\,q(\mathbf{x}')K_0\left(\frac{|\mathbf{x}-\mathbf{x}'|}{R}\right), \qquad \text{(A10)}$$

where $d\mathbf{x}=dx_1dx_2$ and $K_n(\xi)$ denotes a modified Bessel function of nth order [20].

To convert Eq. (A10) into a contour integral, we make use of the equality

$$K_0=R^2\Delta K_0+2\pi R^2\delta(\mathbf{x}-\mathbf{x}')=4R^2\frac{\partial^2K_0}{\partial\bar{z}\partial z}+2\pi R^2\delta(\mathbf{x}-\mathbf{x}'),$$

which follows immediately from the definition of Green's function. Assuming that $\mathbf{x}\to\hat{\mathbf{x}}$, being outside of the region D, and integrating Eq. (A10) by parts, with obvious transformations, we find

$$\hat{\psi}(s) = -\frac{2R^2}{\pi}\int d\mathbf{x}' q(\mathbf{x}')\frac{\partial^2}{\partial\overline{z}'\partial z'}K_0\left(\frac{|\mathbf{x}-\mathbf{x}'|}{R}\right)$$
$$= \frac{2q_0R^2}{\pi}\int d\mathbf{x}'\frac{\partial\theta'}{\partial\overline{z}'}\frac{\partial}{\partial z'}K_0\left(\frac{|\hat{\mathbf{x}}-\mathbf{x}'|}{R}\right)$$
$$= \frac{Rq_0}{2\pi}\int ds' K_1\left(\frac{|\hat{z}'-\hat{z}|}{R}\right)\frac{\hat{z}'_s(\overline{z}'-\overline{z})}{|\hat{z}'-\hat{z}'|}. \quad \text{(A11)}$$

Now we introduce the new variable $\varphi(s)$—the slope angle—the unit vector tangential to the contour at a point s makes with the axis x_1. Then, according to Eq. (A5), we have

$$\partial_s\hat{z} = e^{i\varphi(s)}. \quad \text{(A12)}$$

Let the following be vortex structures with a ''weak contour curvature'':

$$|\kappa| = |\partial_s\varphi| \ll 1/R. \quad \text{(A13)}$$

In this case, it is possible to make the radical approximations in the integral of Eq. (A11),

$$|\hat{z}'-\hat{z}| \approx |s'-s|, \quad \mathrm{Im}\,\hat{z}'_s(\overline{z}'-\overline{z}) \approx \tfrac{1}{2}\kappa(s)(s'-s)^2. \quad \text{(A14)}$$

Here, the overbar denotes complex conjugation.

Using Eq. (A14), the integral (A11) can be reduced to the *local* relation

$$\hat{\psi}(s) = \frac{q_0R^3}{4}\kappa(s), \quad \text{(A15)}$$

which relates the stream function $\hat{\psi}$ and the contour curvature κ in the point s. In the work [22], a ''stream-function''-curvature relation analogous to Eq. (A15) is derived using a different formalism.

APPENDIX B: EQUATION FOR CURVATURE

Let

$$\hat{z} = e^{i\varphi}(\hat{x}+i\hat{y}), \quad \text{(B1)}$$

where $\hat{x}$ and $\hat{y}$ as well as φ are some functions of the contour arc length s. From Eq. (A12) the following relationships hold:

$$\frac{\partial\hat{x}}{\partial s} - \kappa\hat{y} = 1, \quad \frac{\partial\hat{y}}{\partial s} + \kappa\hat{x} = 0. \quad \text{(B2)}$$

Substituting Eqs. (A15) and (B1) in Eq. (A9), we obtain

$$\frac{q_0R^3}{2\omega}\kappa - (\hat{x}^2+\hat{y}^2) = \text{const}. \quad \text{(B3)}$$

We take the length scale $d=(R/2)(q_0/\omega)^{1/3}$. In terms of the dimensionless variables, from Eq. (B2) and Eq. (B3) without changing the old symbol designations, we obtain the equations

$$\frac{\partial\hat{x}}{\partial s} - \kappa\hat{y} = 1, \quad \frac{\partial\hat{y}}{\partial s} + \kappa\hat{x} = 0,$$
$$\kappa - \tfrac{1}{4}(\hat{x}^2+\hat{y}^2) = \text{const}. \quad \text{(B4)}$$

The expressions for variables $\hat{x}$ and $\hat{y}$ in terms of curvature are obtained from Eq. (B4):

$$\hat{x} = 2\frac{\partial\kappa}{\partial s}, \quad \hat{y} = 2c_1 - \kappa^2. \quad \text{(B5)}$$

The substitution (B5) in Eq. (B4) gives the equation for the normalized curvature:

$$\left(\frac{\partial\kappa}{\partial s}\right)^2 = -\frac{1}{4}\kappa^4 + c_1\kappa^2 + \kappa + c_2. \quad \text{(B6)}$$

Here c_1 and c_2 are two constants parametrizing the solutions of the problem. Recall that the condition for application of Eq. (B6) is determined by the inequality (A13), which in dimensionless form is given by

$$|\kappa| \ll \frac{d}{R} = \frac{1}{2}\left|\frac{q_0}{\omega}\right|^{1/3}. \quad \text{(B7)}$$

As the inequality (B7) shows, the condition of weak contour curvature does not limit physical applicability of the solutions as might much appear at first sight. Let recall that a, $d \gg R$. The reason is that the inequality (B7) holds always for intense vortices characterized by large enough values of the ratio q_0/ω.

[1] *Venus*, edited by D. M. Hunten, L. Colin, T. M. Donahue, and V. I. Moroz (The University of Arizona Press, Arizona, 1983), p. 1143.
[2] G. S. Golitsyn, Icarus **13**, 1 (1970).
[3] G. S. Golitsyn, Icarus **60**, 289 (1984).
[4] G. Schubert *et al.*, J. Geophys. Res., [C: Oceans Atmos.] **85**, 8007 (1980).
[5] G. Schubert, in *Venus* (Ref. [1]), p. 1143.
[6] V. V. Kerzhanovich, M. Ya. Marov, and V. I. Moroz, Preprint-831, Space Research Institute (unpublished).
[7] F. W. Taylor *et al.*, J. Geophys. Res., C: Oceans Atmos. **85**, 7963 (1980).
[8] V. M. Linkin *et al.*, Cosmic Res. **23**, 248 (1985).
[9] M. Newman, G. Schubert, A. Kliore, and I. Patel, J. Atmos. Sci. **41**, 1901 (1984).
[10] C. Leovy, J. Atmos. Sci. **30**, 1218 (1973).
[11] O. I. Yakovlev *et al.*, Cosmic Res. **25**, 275 (1987).
[12] O. I. Yakovlev, S. S. Matyugov, and V. N. Gubenko, Cosmic Res. **26**, 762 (1988).
[13] V. M. Gryanik, Sov. Phys. Dokl. **35**, 592 (1990).

[14] V. P. Goncharov and V. I. Pavlov, JETP **92**, 594 (2001).
[15] H. P. Greenspan, *The Theory of Rotating Fluids* (Cambridge University Press, Cambridge, 1968).
[16] J. S. Turner, *Buoyancy Effects in Fluids* (Cambridge University Press, Cambridge, 1979), p. 368.
[17] L. D. Landau and E. M. Lifshitz, *Fluid Mechanics*, 2nd ed. (Pergamon, Oxford, 1987).
[18] V. P. Goncharov and V. I. Pavlov, Phys. Fluids **10**, 2384 (1998).
[19] V. P. Goncharov and V. I. Pavlov, Eur. J. Mech. B/Fluids **19**, 831 (2000).
[20] *Handbook of Mathematical Functions*, edited by M. Abramovitz and I. A. Stegun (U.S. GPO, Washington, D.C., 1964).
[21] E. Madelung, *Die Mathematischen Hilfsmittel Des Physikers* (Springer-Verlag, Berlin, 1957).
[22] A. V. Gruzinov, JETP Lett. **55**, 75 (1992).